Science Advances
AAAS

Supplementary Materials for

Archean cratonic mantle recycled at a mid-ocean ridge

Chuan-Zhou Liu *et al.*

Corresponding author: Chuan-Zhou Liu, chzliu@mail.iggcas.ac.cn

Sci. Adv. **8**, eabn6749 (2022)
DOI: 10.1126/sciadv.abn6749

The PDF file includes:

Figs. S1 to S13
Legends for tables S1 to S5
References

Other Supplementary Material for this manuscript includes the following:

Tables S1 to S5

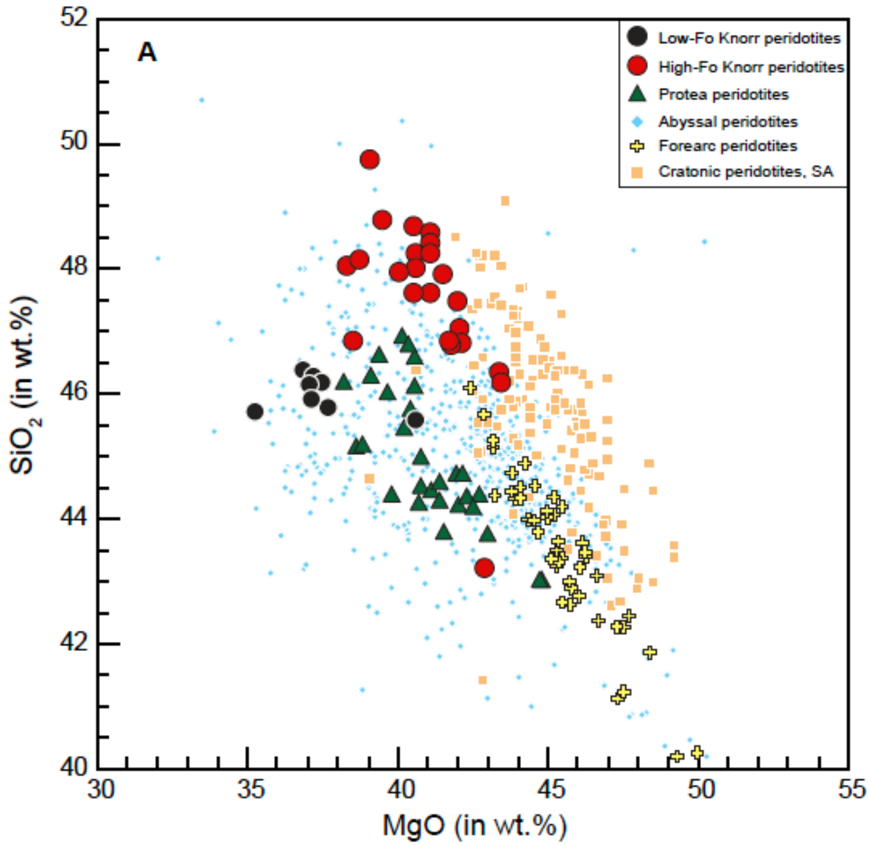

fig. S1. Whole-rock MgO vs SiO_2 contents. The data have been recalculated on an anhydrous basis. Data for abyssal peridotites and the South African (SA) cratonic peridotites are from the PetDB database (http://www.earthchem.org/petdb) and those for forearc peridotites are from refs (*23*, *24*).

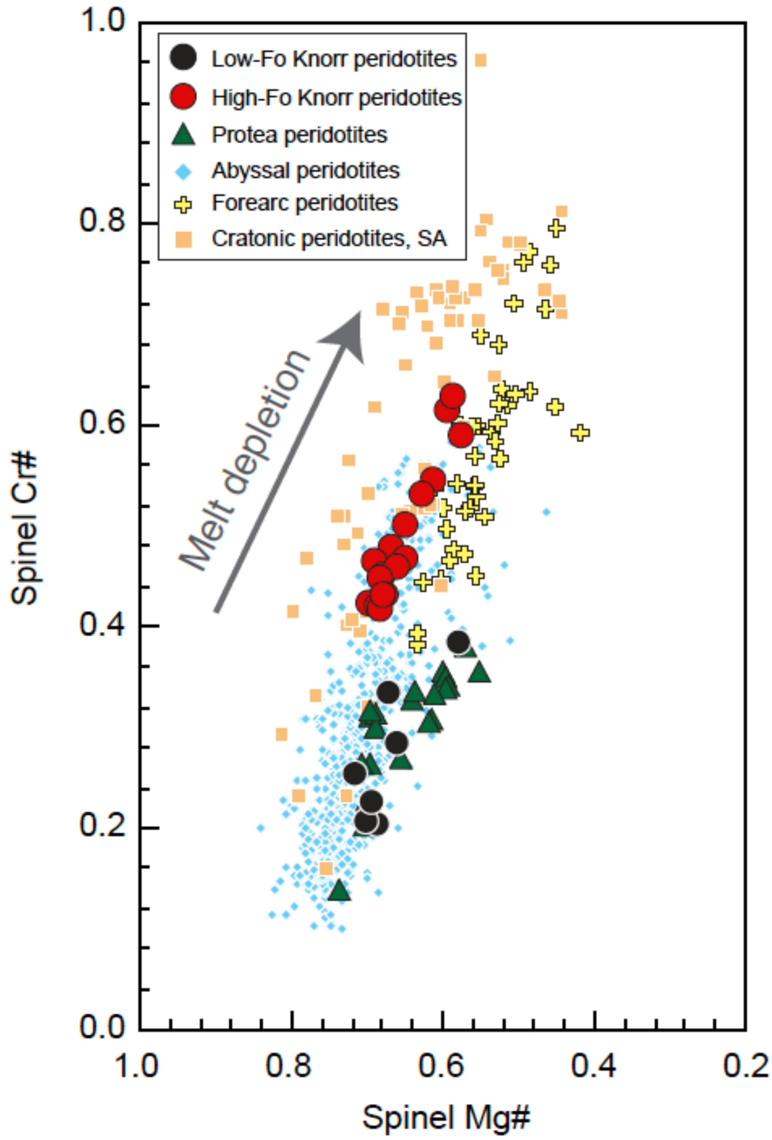

fig. S2. Spinel Mg# versus Cr# values. Data for abyssal peridotites and the South African (SA) cratonic peridotites are from the PetDB database (http://www.earthchem.org/petdb) and those for forearc peridotites are from refs (*23*, *24*).

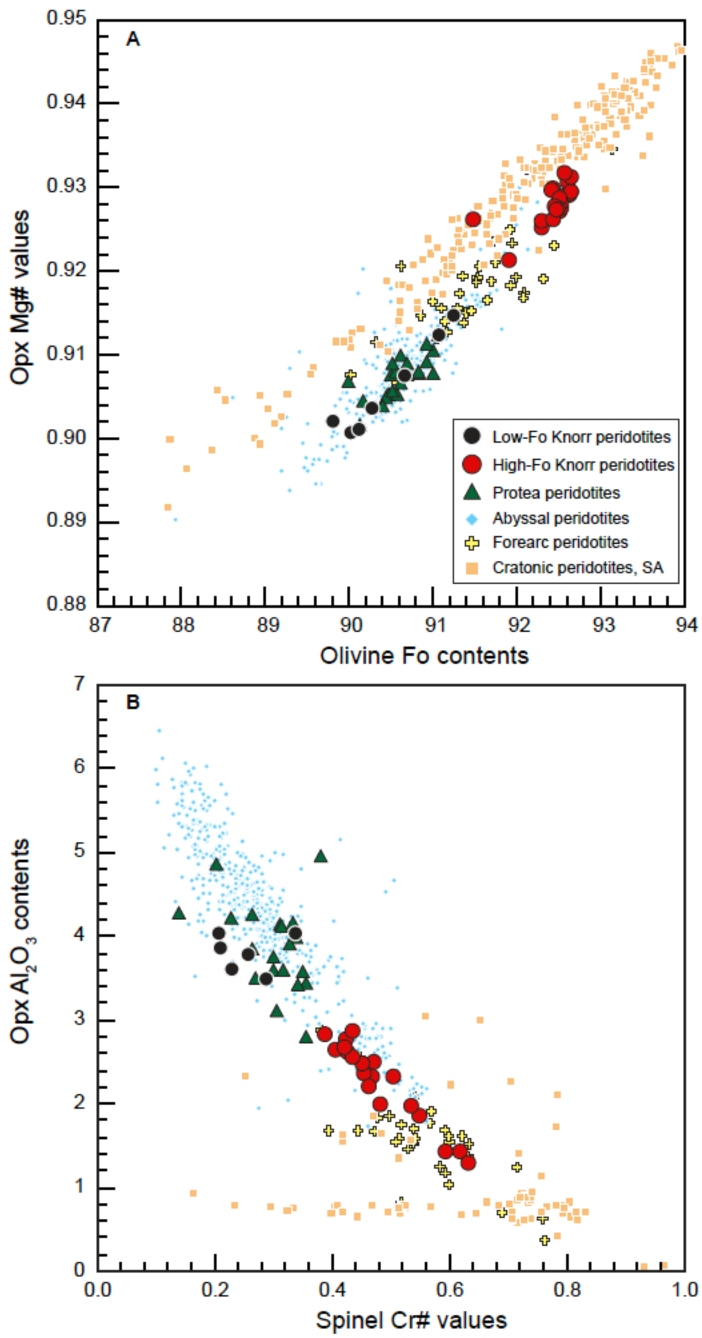

fig. S3. Mineral major elements. (A) Olivine Fo contents versus orthopyroxene Mg#. **(B)** Spinel Cr# values versus orthopyroxene Al_2O_3 contents. Data for abyssal peridotites and the South African (SA) cratonic peridotites are from the PetDB database (http://www.earthchem.org/petdb) and those for forearc peridotites are from refs (*23*, *24*).

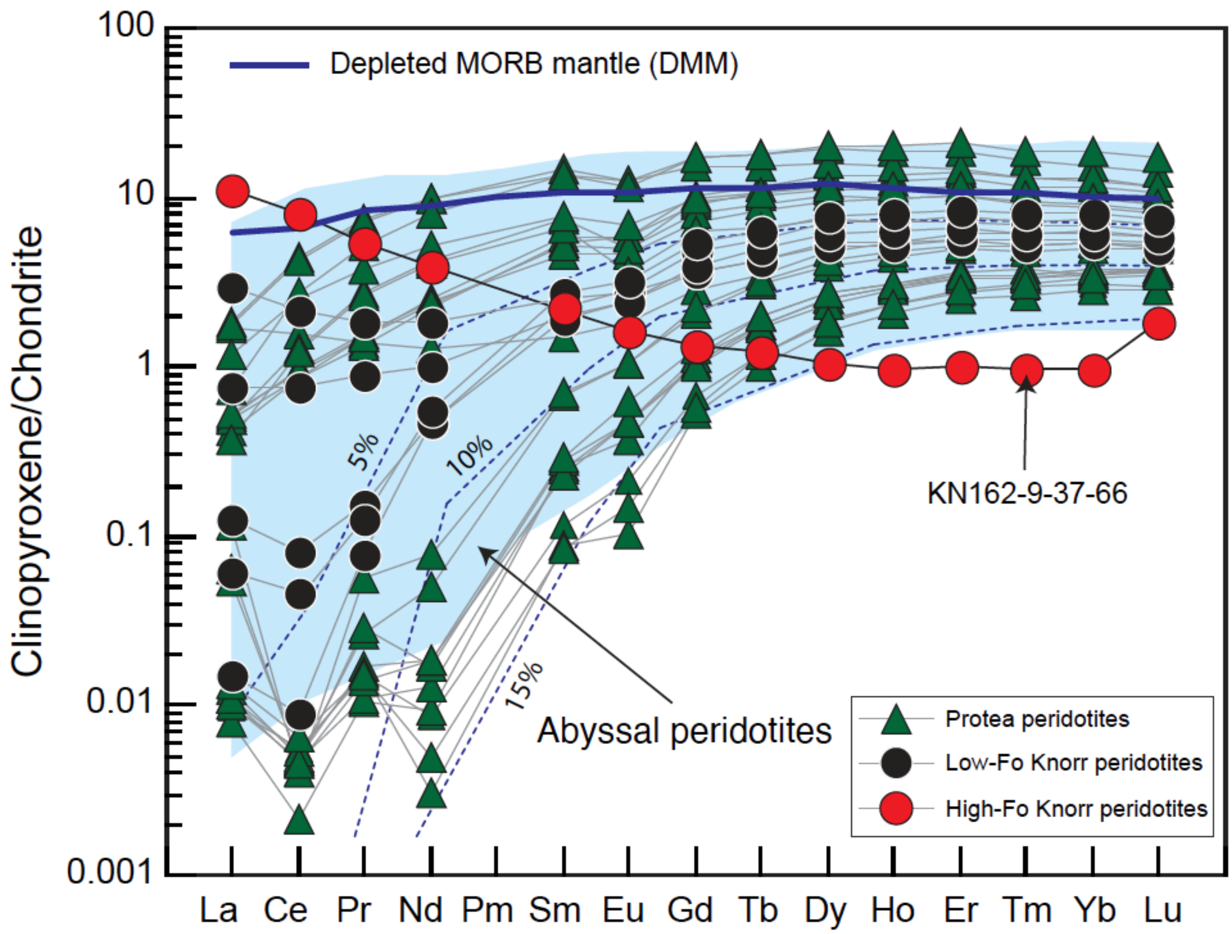

fig. S4. Rare earth element (REE) patterns of clinopyroxenes. Clinopyroxene is normalized to CI chondrites, using values from ref. (*18*). Clinopyroxene of the depleted MORB mantle (DMM) is from ref. (*63*). The field of abyssal peridotites is from ref. (*14*).

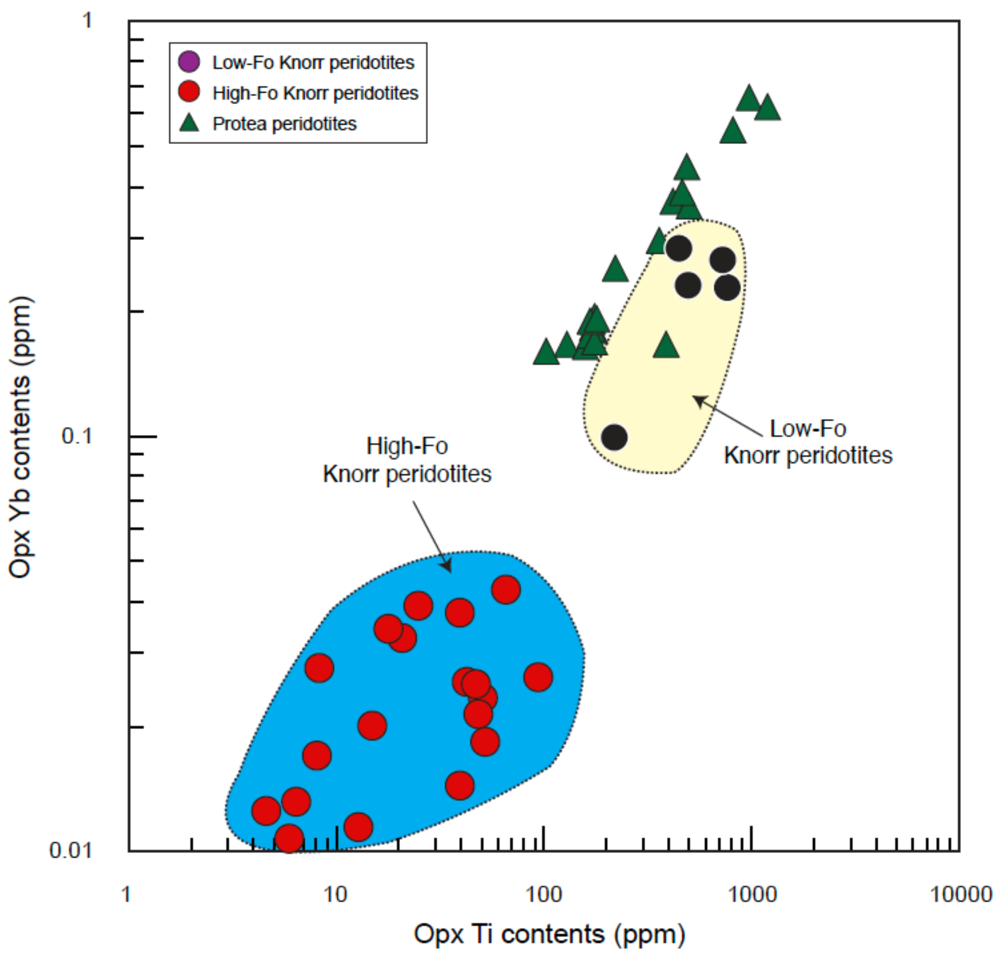

fig. S5. Orthopyroxene Ti versus Yb contents.

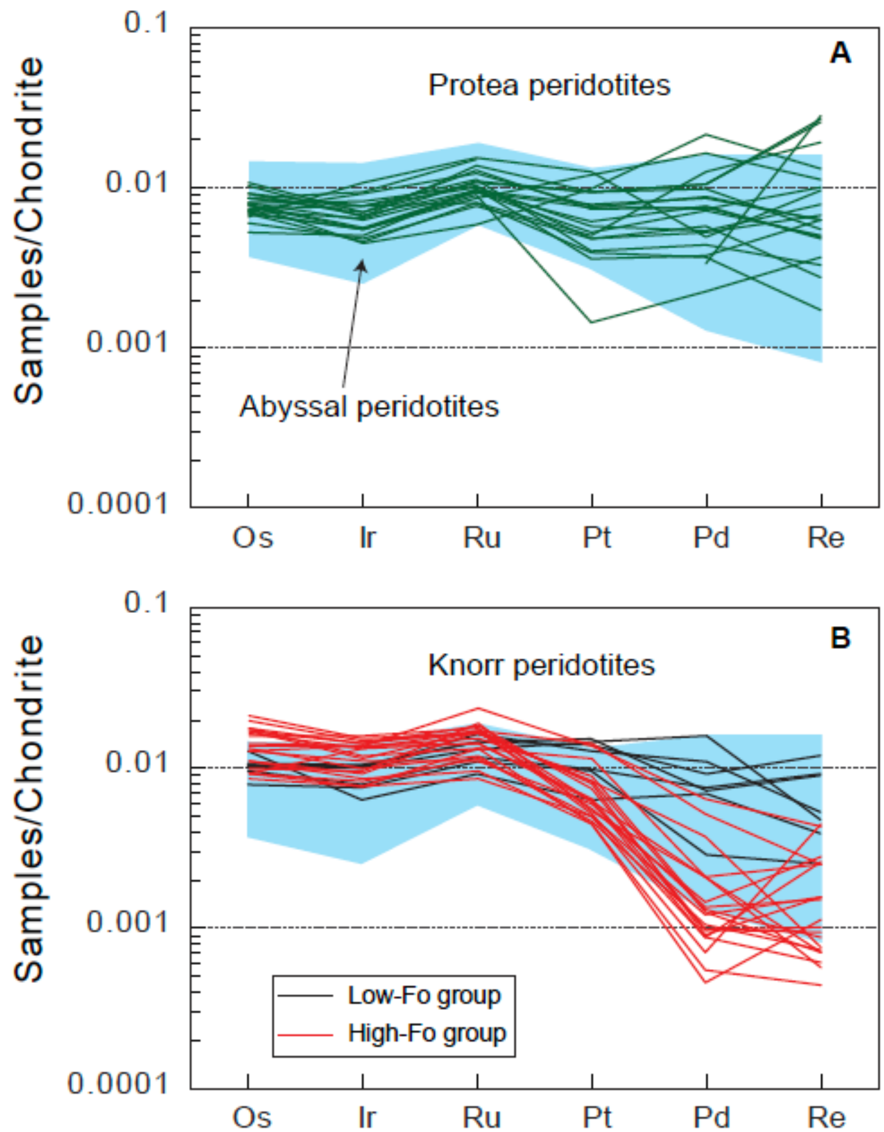

fig. S6. Highly siderophile element patterns. Samples (**A**) Dredge haul PROT5 and (**B**) Dredge haul KN162-9. Data for abyssal peridotites are from refs (*8, 19*). Chondritic values are from ref. (*56*).

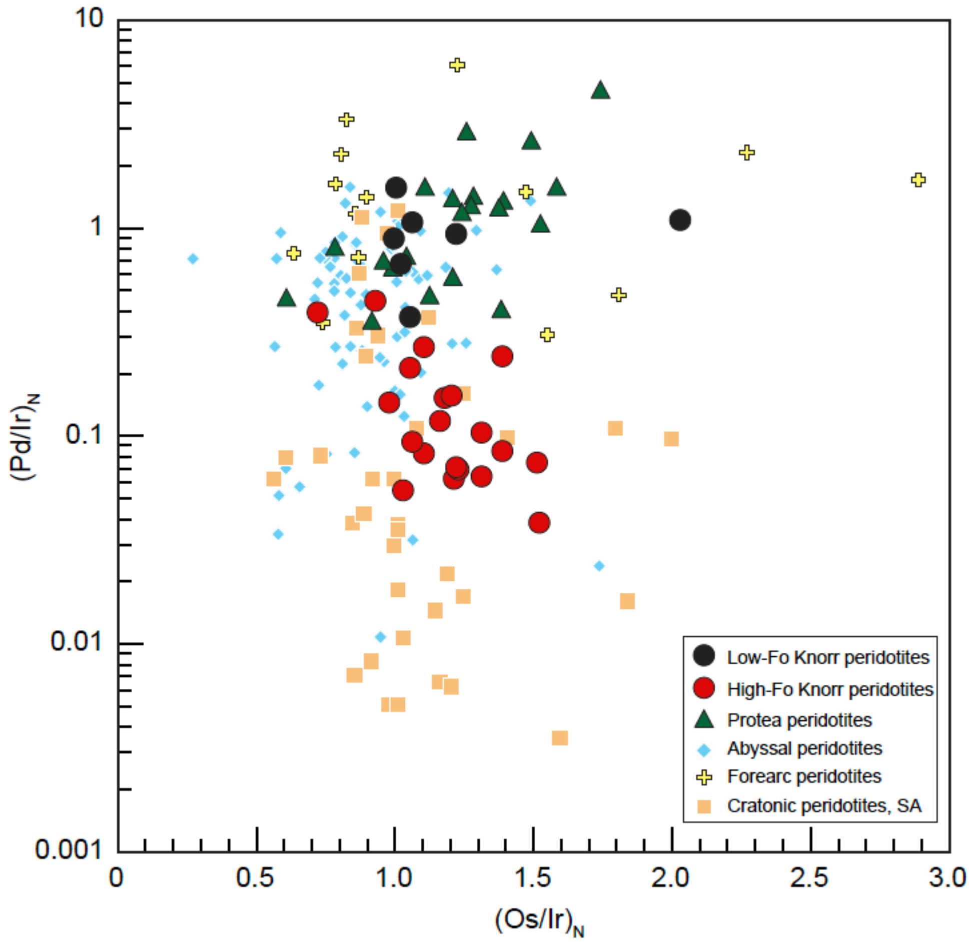

fig. S7. Os/Ir versus Pd/Ir ratios. Data of abyssal peridotites (*8, 18, 57*), South African cratonic peridotites (*19*) and forearc peridotites are shown for comparison.

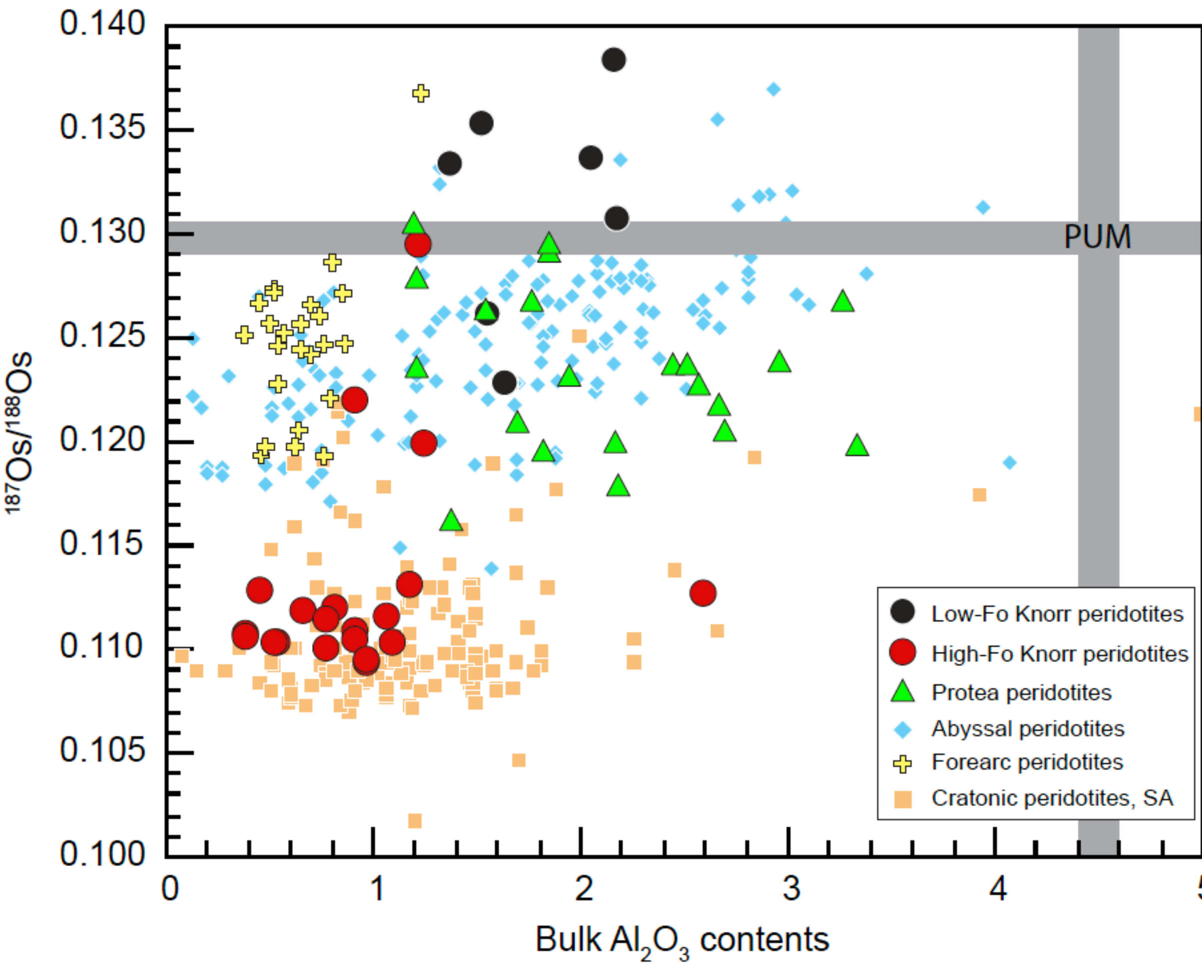

fig. S8. Bulk Al_2O_3 contents versus $^{187}Os/^{188}Os$ ratios. Data sources by lithology include abyssal peridotites (*2-5, 8, 21, 57*), forearc peridotites (*24, 58*), and South African mantle xenoliths (*19, 59-67*). The SWIR peridotites with $^{187}Os/^{188}Os$ ratios higher than those of the PUM might be due to melt refertilization or interaction with seawater (*21*).

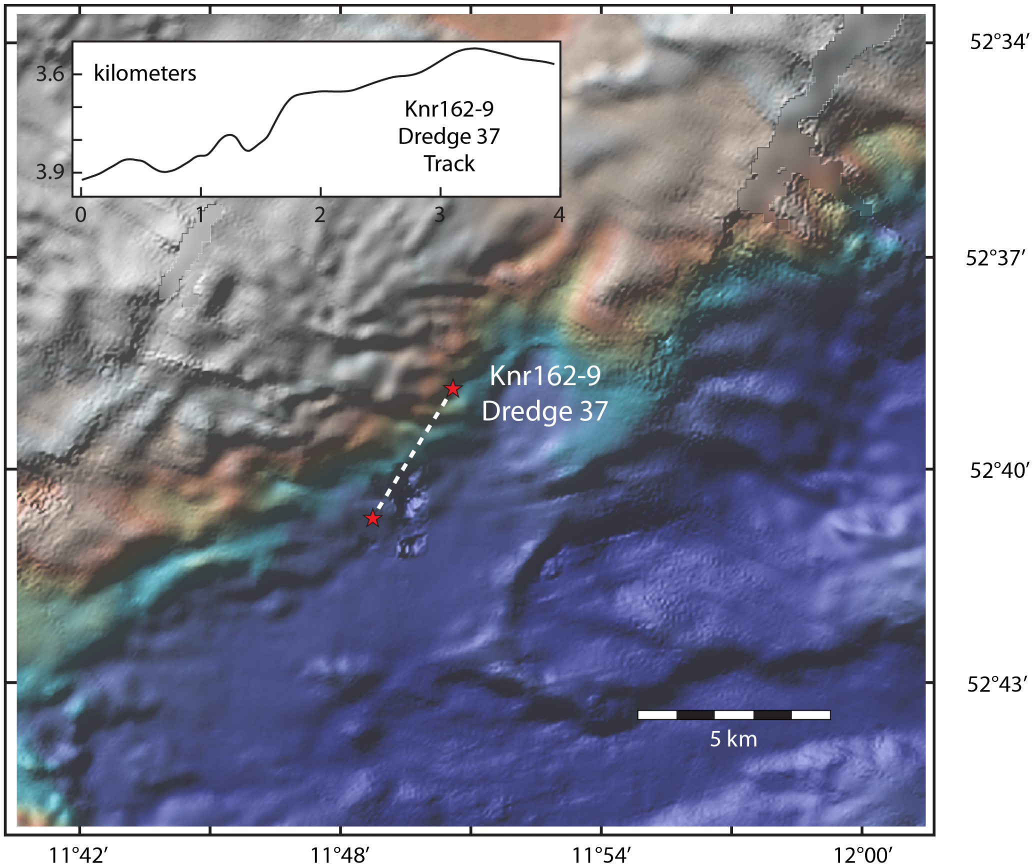

fig. S9. Colored relief map of the Dredge 37 location. The beginning and end points are shown as red stars, and the track itself as a dashed white line. Inset shows the bathymetric relief over the length of the track with both vertical and horizontal scales in kilometer.

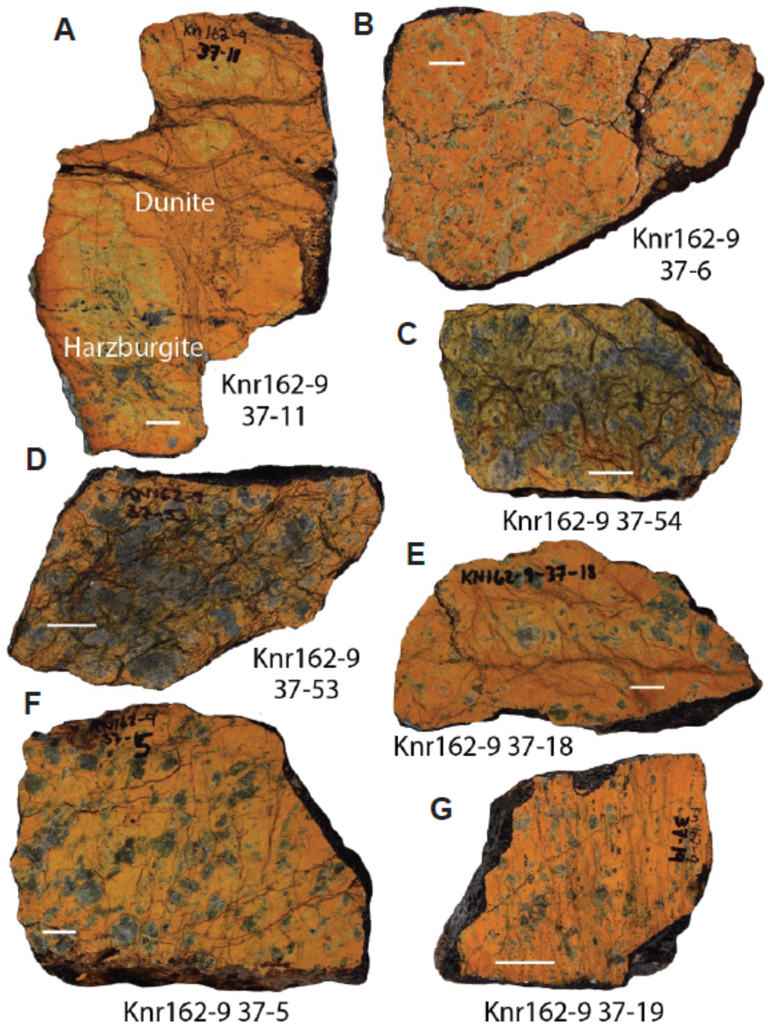

fig. S10. Representative examples of Dredge 37 peridotites with different textures. (A) A chrome spinel bearing dunite with a patch of harzburgite representing a diffuse contact between these lithologies; **(B)** a pervasive altered harzburgite; **(C)** One relatively fresh peridotite contains an irregular ~0.5 mm vein of fresh plagioclase; **(D)** a pyroxene-rich lherzolite; **(E)** a pyroxene-poor harzburgite; **(F)** a harzburgite with a visible foliation defined by rounded and stretched pyroxenes; **(G)** a harzburgite with 1-2 mm rounded relict pyroxenes and a clear foliation. Typical grain size for the peridotites is close to 0.4 mm, but Knr162-9 37-6 is an atypical medium-grained harzburgite. Textures vary from protogranular with deeply embayed and lobed pyroxene grain boundaries **(C)**, porphyroclastic with a visible foliation defined by rounded and stretched pyroxenes **(F)**, to protomylonitic with 1-2 mm rounded relict pyroxenes and a clear foliation **(G)**. Modal proportions range from about 12 to 30 vol.% pyroxene. While the pyroxene is relatively evenly distributed in many of the samples, (e.g., **B-D, F**), in others the pyroxene is irregularly distributed (**A, E**). The white bars are 1 cm scales.

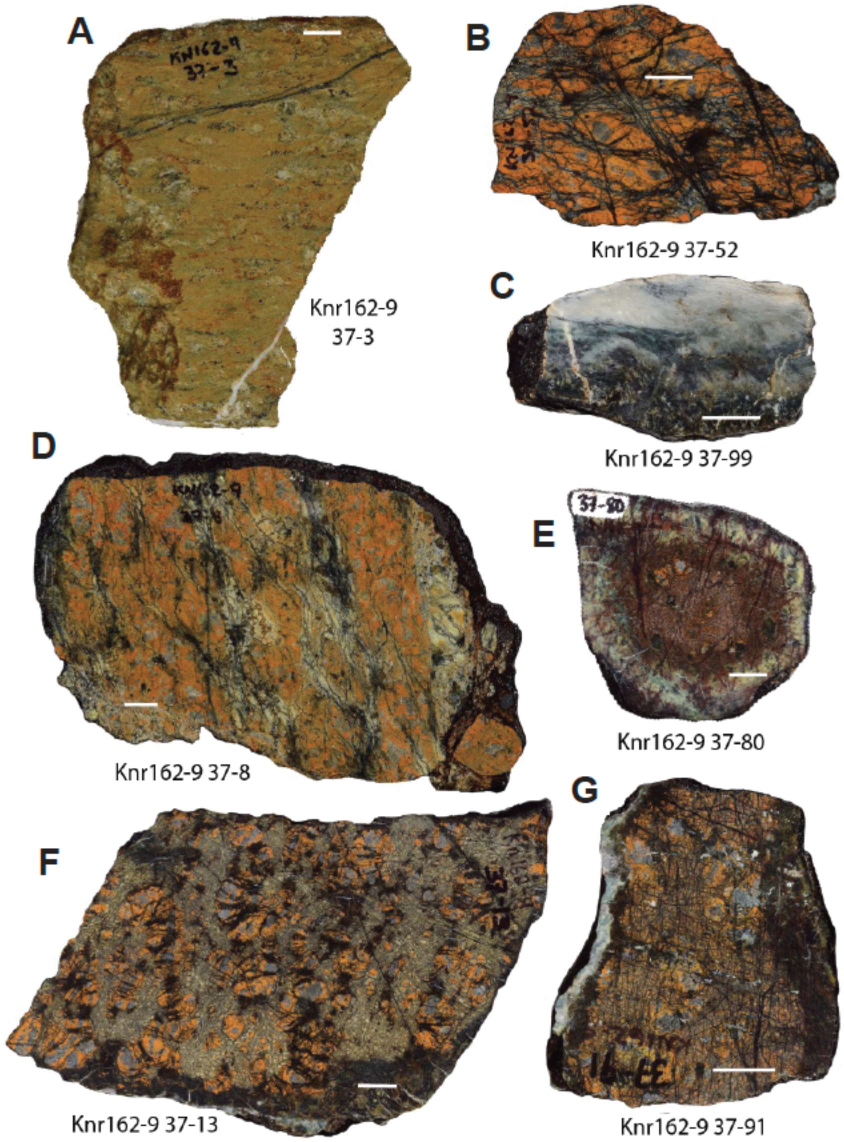

fig. S11. Representative samples from Dredge 37 showing variable degrees of alteration. A late stage deformation is associated with serpentine shear zones.

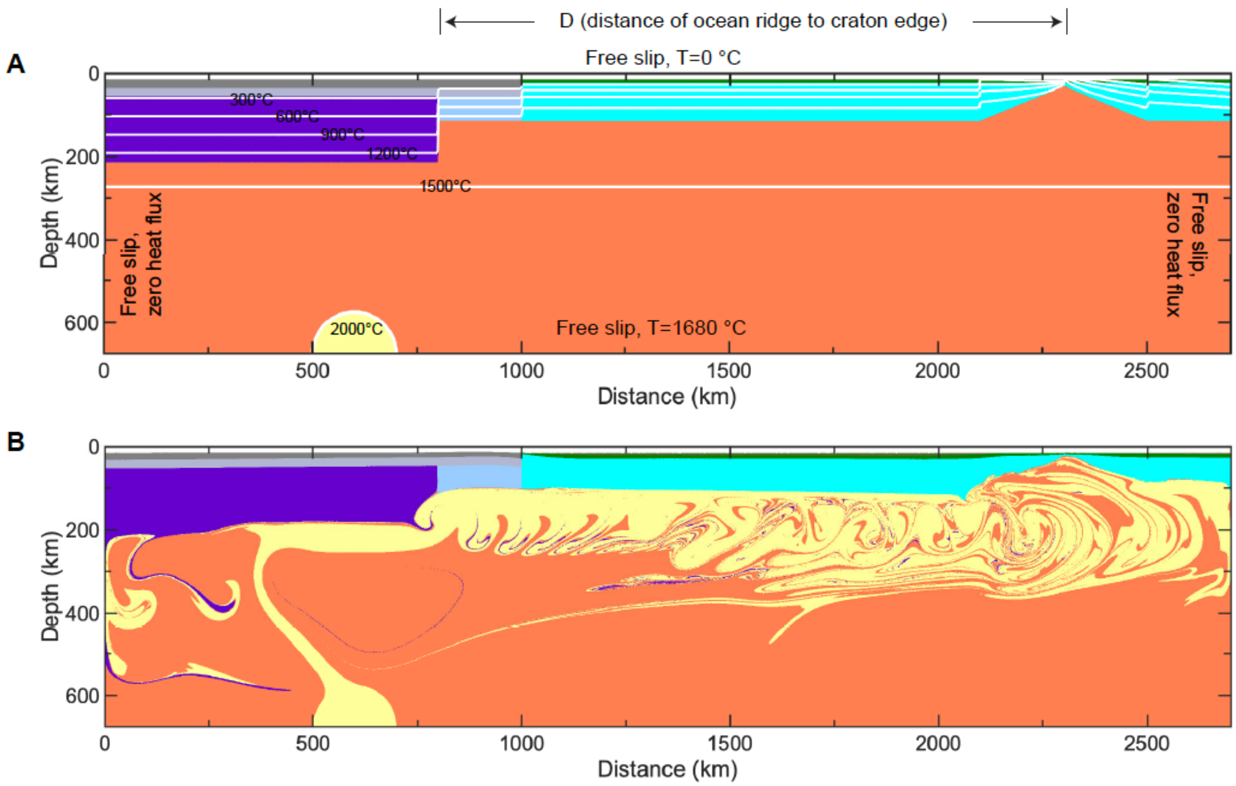

fig. S12. Additional model results. (A) Initial model set-up. The white lines denote temperature contours. **(B)** Composition field for a relatively higher resolution of 901×451 nodes.

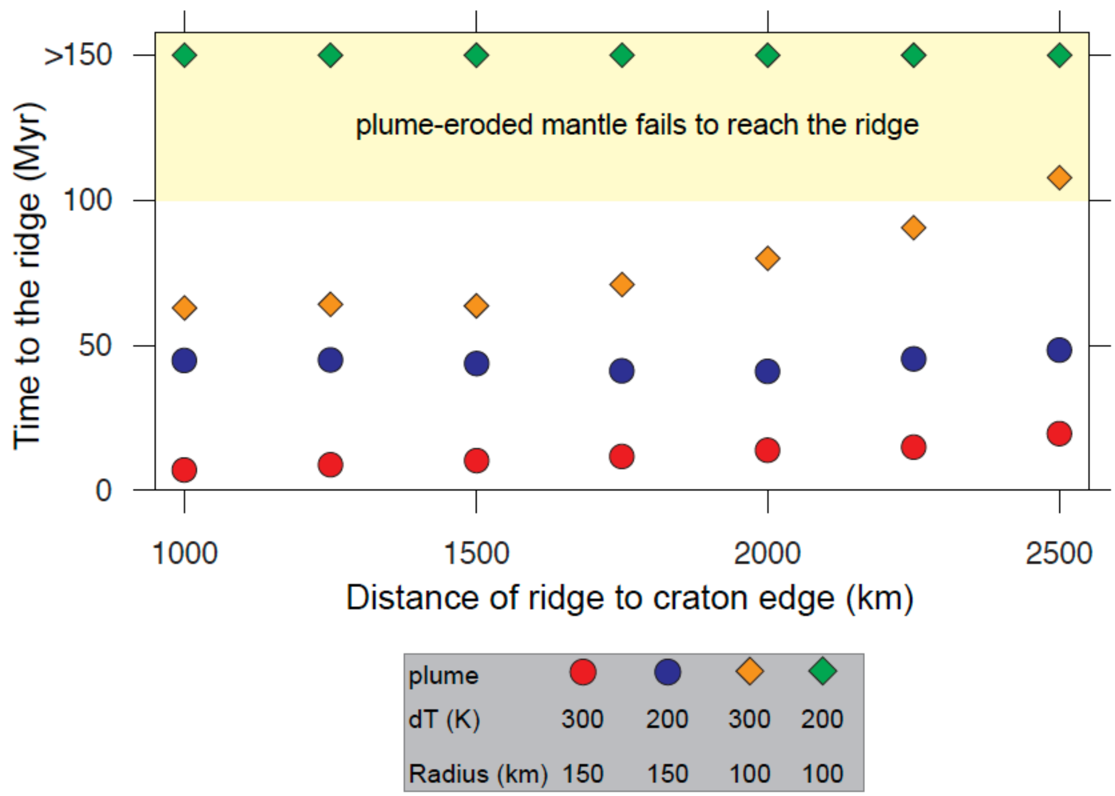

fig. S13. Systematic models of different plume radius and excess temperature versus the time of cratonic lithosphere flowing to the ridge. A radius of 100 km with an excess temperature of 300 K for the plume is used for the reference model shown in Figure 4. Note that the ">150 Myr" (million years) indicates that the cratonic material cannot reach the ridge when the plume is too weak (100 km in radius and 200 K in excess temperature).

Table S1

Whole rock major elements of the SWIR peridotites

Table S2

Mineral major elements of the SWIR peridotites

Table S3

Trace elements of clinopyroxene and orthopyroxenes in the SWIR peridotites

Table S4

Highly siderophile elements and Re-Os isotopes of the SWIR peridotites

Table S5

Physical properties of rocks used for the numerical modelling

REFERENCES AND NOTES

1. A. Zindler, S. Hart, Chemical geodynamics. *Annu. Rev. Earth Planet. Sci.* **14**, 493–571 (1986).

2. A. D. Brandon, J. E. Snow, R. J. Walker, J. W. Morgan, T. D. Mock, ^{190}Pt–^{186}Os and ^{187}Re–^{187}Os systematics of abyssal peridotites. *Earth Planet. Sci. Lett.* **177**, 319–335 (2000).

3. J. Harvey, A. Gannoun, K. W. Burton, N. W. Rogers, O. Alard, I. J. Parkinson, Ancient melt extraction from the oceanic upper mantle revealed by Re–Os isotopes in abyssal peridotites from the Mid-Atlantic ridge. *Earth Planet. Sci. Lett.* **244**, 606–621 (2006).

4. J. C. Lassiter, B. L. Byerly, J. E. Snow, E. Hellebrand, Constraints from Os-isotope variations on the origin of Lena Trough abyssal peridotites and implications for the composition and evolution of the depleted upper mantle. *Earth Planet. Sci. Lett.* **403**, 178–187 (2014).

5. C. Z. Liu, J. E. Snow, E. Hellebrand, G. Brügmann, A. von der Handt, A. Büchl, A. W. Hofmann, Ancient, highly heterogeneous mantle beneath Gakkel ridge, Arctic Ocean. *Nature* **452**, 311–316 (2008).

6. A. V. Sobolev, N. Shimizu, Ultra-depleted primary melt included in an olivine from the Mid-Atlantic Ridge. *Nature* **363**, 151–154 (1993).

7. A. Stracke, F. Genske, J. Berndt, J. M. Koornneef, Ubiquitous ultra-depleted domains in Earth's mantle. *Nat. Geosci.* **12**, 851–855 (2019).

8. J. M. D. Day, R. J. Walker, J. M. Warren, ^{186}Os–^{187}Os and highly siderophile element abundance systematics of the mantle revealed by abyssal peridotites and Os-rich alloys. *Geochim. Cosmochim. Acta* **200**, 232–254 (2017).

9. A. Stracke, J. E. Snow, E. Hellebrand, A. von der Handt, B. Bourdon, K. Birbaum, D. Günther, Abyssal peridotite Hf isotopes identify extreme mantle depletion. *Earth Planet. Sci. Lett.* **308**, 359–368 (2011).

10. S. Y. O'Reilly, M. Zhang, W. L. Griffin, G. Begg, J. Hronsky, Ultradeep continental roots and their oceanic remnants: A solution to the geochemical "mantle reservoir" problem? *Lithos* **112**, 1043–1054 (2009).

11. D. G. Pearson, J. M. Scott, J. Liu, A. Schaeffer, L. H. Wang, J. van Hunen, K. Szilas, T. Chacko, P. B. Kelemen, Deep continental roots and cratons. *Nature* **596**, 199–210 (2021).

12. F. Y. Wu, Y. G. Xu, R. X. Zhu, G. W. Zhang, Thinning and destruction of the cratonic lithosphere: A global perspective. *Sci. China-Earth Sci.* **57**, 2878–2890 (2014).

13. H. Y. Zhou, H. J. B. Dick, Thin crust as evidence for depleted mantle supporting the Marion Rise. *Nature* **494**, 195–200 (2013).

14. J. M. Warren, Global variations in abyssal peridotite compositions. *Lithos* **248-251**, 193–219 (2016).

15. E. Hellebrand, J. E. Snow, H. J. B. Dick, A. W. Hofmann, Coupled major and trace elements as indicators of the extent of melting in mid-ocean-ridge peridotites. *Nature* **410**, 677–681 (2001).

16. E. Anders, N. Grevesse, Abundances of the elements: Meteoritic and solar. *Geochim. Cosmochim. Acta* **53**, 197–214 (1989).

17. D. G. Pearson, D. Canil, S. B. Shirey, in *Treatise on Geochemistry,* H. D. Holland, K. K. Turekian, Eds. (Elsevier, 2014), vol. 3, pp. 169–253.

18. C. Z. Liu, J. E. Snow, G. Brügmann, E. Hellebrand, A. W. Hofmann, Non-chondritic HSE budget in Earth's upper mantle evidenced by abyssal peridotites from Gakkel ridge (Arctic Ocean). *Earth Planet. Sci. Lett.* **283**, 122–132 (2009).

19. D. G. Pearson, G. J. Irvine, D. A. Ionov, F. R. Boyd, G. E. Dreibus, Re–Os isotope systematics and platinum group element fractionation during mantle melt extraction: A study of massif and xenolith peridotite suites. *Chem. Geol.* **208**, 29–59 (2004).

20. T. Meisel, R. J. Walker, A. J. Irving, J.-P. Lorand, Osmium isotopic compositions of mantle xenoliths: A global perspective. *Geochim. Cosmochim. Acta* **65**, 1311–1323 (2001).

21. J. E. Snow, L. Reisberg, Os isotopic systematics of the MORB mantle: Results from altered abyssal peridotites. *Earth Planet. Sci. Lett.* **133**, 411–421 (1995).

22. R. L. Rudnick, R. J. Walker, Interpreting ages from Re–Os isotopes in peridotites. *Lithos* **112**, 1083–1095 (2009).

23. I. J. Parkinson, J. A. Pearce, Peridotites from the Izu-Bonin-Mariana forearc (ODP leg 125): Evidence for mantle melting and melt-mantle interaction in a supra-subduction zone setting. *J. Petrol.* **39**, 1577–1618 (1998).

24. J. M. D. Day, D. B. Brown, Ancient melt-depletion in fresh to strongly serpentinized Tonga trench peridotites. *J. Petrol.* **62**, egab088 (2021).

25. F. R. Boyd, N. P. Pokhilenko, D. G. Pearson, S. A. Mertzman, N. V. Sobolev, L. W. Finger, Composition of the Siberian cratonic mantle: Evidence from Udachnaya peridotite xenoliths. *Contri. Mineral. Petrol.* **128**, 228–246 (1997).

26. A. Tuck-Martin, J. Adam, G. Eagles, New plate kinematic model and tectono-stratigraphic history of the East African and West Madagascan Margins. *Basin Res.* **30**, 1118–1140 (2018).

27. R. W. Carlson, D. G. Pearson, D. E. James, Physical, chemical, and chronological characteristics of continental mantle. *Rev. Geophys.* **43**, RG1001 (2005).

28. F. Y. Wu, J. H. Yang, Y. G. Xu, S. A. Wilde, R. J. Walker, Destruction of the North China Craton in the Mesozoic. *Annu. Rev. Earth Planet. Sci.* **47**, 173–195 (2019).

29. S. Y. O'Reilly, W. L. Griffin, Y. H. Poudjom Djomani, Are lithospheres forever? Tracking changes in subcontinental lithospheric mantle through time. *GSA Today* **11**, 4–10 (2001).

30. J. Hu, L. Liu, M. Faccenda, Q. Zhou, K. M. Fischer, S. Marshak, C. Lundstrom, Modification of the Western Gondwana craton by plume–lithosphere interaction. *Nat. Geosci.* **11**, 203–210 (2018).

31. C. T. A. Lee, P. Luffi, E. J. Chin, Building and destroying continental mantle. *Annu. Rev. Earth Planet. Sci.* **39**, 59–90 (2011).

32. R. L. Armstrong, Radiogenic isotopes: The case for crustal recycling on a near-steadystate no-continental-growth Earth. *Phil. Trans. R. Soc. Lond. A* **301**, 443–472 (1981).

33. B. Dhuime, C. J. Hawkesworth, P. A. Cawood, C. D. Storey, A change in the geodynamics of continental growth 3 billion years ago. *Science* **335**, 1334–1336 (2012).

34. M. Guo, J. Korenaga, Argon constraints on the early growth of felsic continental crust. *Sci. Adv.* **6**, eaaz6234 (2020).

35. W. L. Griffin, S. Y. O'Reilly, N. Abe, S. Aulbach, R. M. Davies, N. J. Pearson, B. J. Doyle, K. Kivi, The origin and evolution of Archean lithospheric mantle. *Precambrian Res.* **127**, 19–41 (2003).

36. M. D. Behn, C. P. Conrad, P. G. Silver, Detection of upper mantle flow associated with the African Superplume. *Earth Planet. Sci. Lett.* **224**, 259–274 (2004).

37. M. Tsekhmistrenko, K. Sigloch, K. Hosseini, G. Barruol, A tree of Indo-African mantle plumes imaged by seismic tomography. *Nat. Geosci.* **14**, 612–619 (2021).

38. S. F. Foley, Rejuvenation and erosion of the cratonic lithosphere. *Nat. Geosci.* **1**, 503–510 (2008).

39. B. M. Urann, H. J. B. Dick, R. Parnell-Turner, J. F. Casey, Recycled arc mantle recovered from the Mid-Atlantic Ridge. *Nat. Commun.* **11**, 3887 (2020).

40. I. H. Campbell, R. W. Griffiths, R. I. Hill, Melting in an Archaean mantle plume: Heads it's basalts, tails it's komatiites. *Nature* **339**, 697–699 (1989).

41. C. J. Spencer, Continuous continental growth as constrained by the sedimentary record. *Am. J. Sci.* **320**, 373–401 (2020).

42. H. J. B. Dick, J. Lin, H. Schouten, An ultraslow-spreading class of ocean ridge. *Nature* **426**, 405–412 (2003).

43. J. J. Standish, H. J. B. Dick, P. J. Michael, W. G. Melson, T. O'Hearn, MORB generation beneath the ultraslow spreading Southwest Indian Ridge (9–25°E): Major element chemistry and the importance of process versus source. *Geochem. Geophys. Geosys.* **9**, 1–39 (2008).

44. J. E. Georgen, J. Lin, H. J. B. Dick, Evidence from gravity anomalies for interactions of the Marion and Bouvet hotspots with the Southwest Indian Ridge: Effects of transform offsets. *Earth Planet. Sci. Lett.* **187**, 283–300 (2001).

45. C. M. Meyzen, J. Blichert-Toft, J. N. Ludden, E. Humler, C. Mével, F. Albarède, Isotopic portrayal of the Earth's upper mantle flow field. *Nature* **447**, 1069–1074 (2007).

46. Z.-Y. Chu, F. Y. Wu, R. J. Walker, R. L. Rudnick, L. Pitcher, I. S. Puchtel, Y. H. Yang, S. A. Wilde, Temporal evolution of the lithospheric mantle beneath the eastern north china craton. *J. Petrol.* **50**, 1857–1898 (2009).

47. J. L. Birck, M. Roy-Barman, F. Capmas, Re-Os isotopic measurements at the femtomole level in natural samples. *Geostandard. Newslett.* **21**, 19–27 (1997).

48. S. B. Shirey, R. J. Walker, The Re-Os isotope system in cosmochemistry and high-temperature geochemistry. *Annu. Rev. Earth Planet. Sci.* **26**, 423–500 (1998).

49. R. J. Walker, R. W. Carlson, S. B. Shirey, F. R. Boyd, Os, Sr, Nd, and Pb isotope systematics of southern African peridotite xenoliths: Implications for the chemical evolution of subcontinental mantle. *Geochim. Cosmochim. Acta* **53**, 1583–1595 (1989).

50. T. V. Gerya, D. A. Yuen, Characteristics-based marker-in-cell method with conservative finite-differences schemes for modeling geological flows with strongly variable transport properties. *Phys. Earth Planet. Int.* **140**, 293–318 (2003).

51. F. Crameri, H. Schmeling, G. J. Golabek, T. Duretz, R. Orendt, S. J. H. Buiter, D. A. May, B. J. P. Kaus, T. V. Gerya, P. J. Tackley, A comparison of numerical surface topography calculations in geodynamic modelling: An evaluation of the ‘sticky air’ method. *Geophys. J. Int.* **189**, 38–54 (2012).

52. B. J. Kaus, H. Mühlhaus, D. A. May, A stabilization algorithm for geodynamic numerical simulations with a free surface. *Phys. Earth Planet. Inter.* **181**, 12–20 (2010).

53. S. I. Karato, P. Wu, Rheology of the upper mantle: A synthesis. *Science* **260**, 771–778 (1993).

54. J. Van Wijk, J. Van Hunen, S. Goes, Small-scale convection during continental rifting: Evidence from the Rio Grande rift. *Geology* **36**, 575–578 (2008).

55. A. Koptev, E. Calais, E. Burov, S. Leroy, T. Gerya, Dual continental rift systems generated by plume–lithosphere interaction. *Nat. Geosci.* **8**, 388–392 (2015).

56. P. E. Janney, S. B. Shirey, R. W. Carlson, D. G. Pearson, D. R. Bell, A. P. le Roex, A. Ishikawa, P. H. Nixon, F. R. Boyd, Age, composition and thermal characteristics of south african off-craton mantle lithosphere: Evidence for a multi-stage history. *J. Petrol.* **51**, 1849–1890 (2010).

57. R. W. Carlson, R. O. Moore, Age of the Eastern Kaapvaal mantle: Re-Os isotope data for peridotite xenoliths from the Monastery kimberlite. *S. Afr. J. Geol* **107**, 81–90 (2004).

58. R. W. Carlson, J. B. Dawson, P. H. Nixon, in *Proceedings of the 7th International Kimberlite Conference*, J. J. Gurney, Ed. (Cape Town, 1999), pp. 99–108.

59. A. Luguet, M. Behrens, D. G. Pearson, S. König, D. Herwartz, Significance of the whole rock Re–Os ages in cryptically and modally metasomatised cratonic peridotites: Constraints from HSE–Se–Te systematics. *Geochim. Cosmochim. Acta* **164**, 441–463 (2015).

60. A. H. Menzies, R. W. Carlson, S. B. Shirey, J. J. Gurney, in *Proceedings of the 7th International Kimberlite Conference*, J. J. Gurney, Ed. (Cape Town, 1997), pp. 566–573.

61. D. G. Pearson, R. W. Carlson, S. B. Shirey, F. R. Boyd, P. H. Nixon, Stabilisation of Archaean lithospheric mantle: A Re-Os isotope study of peridotite xenoliths from the Kaapvaal craton. *Earth Planet. Sci. Lett.* **134**, 341–357 (1995).

62. N. Simon, The origin of garnet and clinopyroxene in “depleted” Kaapvaal peridotites. *Lithos* **71**, 289–322 (2003).

63. N. S. C. Simon, R. W. Carlson, D. G. Pearson, G. R. Davies, The origin and evolution of the Kaapvaal cratonic lithospheric mantle. *J. Petrol.* **48**, 589–625 (2007).

64. C. B. Smith, D. G. Pearson, G. P. Bulanova, A. D. Beard, R. W. Carlson, N. Wittig, K. Sims, L. Chimuka, E. Muchemwa, Extremely depleted lithospheric mantle and diamonds beneath the southern Zimbabwe Craton. *Lithos* **112**, 1120–1132 (2009).

65. M. F. Horan, R. J. Walker, J. W. Morgan, J. N. Grossman, A. E. Rubin, Highly siderophile elements in chondrites. *Chem. Geol.* **196**, 27–42 (2003).

66. M. Paquet, J. M. D. Day, D. B. Brown, C. L. Waters, Effective global mixing of the highly siderophile elements into Earth’s mantle inferred from oceanic abyssal peridotites. *Geochim. Cosmochim. Acta* **316**, 347–362 (2022).

67. I. J. Parkinson, C. J. Hawkesworth, A. S. Cohen, Ancient mantle in a modern arc: Osmium isotopes in izu-bonin-mariana forearc peridotites. *Science* **281**, 2011–2013 (1998).